Convective instability of an acidity front in Hele-Shaw cells

Tamás Bánsági, Jr., Dezső Horváth, and Ágota Tóth*

Department of Physical Chemistry, University of Szeged, P.O. Box 105, Szeged H-6701, Hungary
(Received 4 April 2003; published 7 August 2003)

Density fingering arising in the acid-catalyzed chlorite-tetrathionate reaction is investigated experimentally in Hele-Shaw cells of various thickness. Upward propagating chemical fronts are stable for all gapwidths examined. The initial evolution of the downward propagating planar fronts resulting in a cellular structure has been characterized by dispersion curves and it is found that the convectively unstable regime increases as the gapwidth increases. From the dispersion curves, the change in the characteristics of the most unstable mode and in the marginal wave number, separating the stable and unstable modes, is determined quantitatively.

I. INTRODUCTION

Convection may play a major role in spatiotemporal pattern formation in addition to diffusion [1]. The fluid motion affects the velocity and the shape of chemical fronts via the orientation of the reaction vessel and the change in the density of the solution in the course of the autocatalytic reaction [2–4]. The density may vary because of the compositional change and—for exothermic reactions—the thermal expansion of the solution. The latter has generally smaller contribution, since experiments are carried out in narrow vessels of various geometry providing sufficient heat removal to the surroundings. Initially the effect of convection on autocatalytic reactions in aqueous solutions has been studied in thin tubes with addressing the variation of front velocity and visually describing the shape of the reaction front as a result of one or two convection rolls forming in the reaction vessel [3,5]. In a Hele-Shaw cell [6], consisting of a thin layer of solution between two planar walls with a small gapwidth, the system is effectively two-dimensional allowing a potential-flow model for fluid dynamics. Experiments carried out in Hele-Shaw cells [7–10], therefore, provide essential data to theories studying the interaction between the hydrodynamic flow and a propagating chemical front. In the iodate-arsenous acid reaction, for example, the arising cellular patterns have a distinct wave number with a well-defined amplitude [8] in accordance with the dispersion relation determined experimentally by Böckmann and Müller [9]. Previously we have investigated quantitatively the effect of orientation on the evolution of cellular patterns at a constant change in density for acid-catalyzed fronts of the chlorite-tetrathionate reaction [10]. We have shown that the high-frequency modes are stabilized by diffusion in the buoyantly unstable orientation and the surface tension at the interface between the reactant and product solutions plays no role in the pattern formation.

The theoretical studies describing the influence of convection on autocatalytic fronts either consider the chemical reaction as an infinitesimally narrow zone separating two solutions of different density [11] or use the full balance equations for the important components—to incorporate chemistry—yielding a continuous variation of density across

the front [12]. For the fluid flow in thin layers of solution, Darcy's law applicable in porous media or the more elaborate Navier-Stokes equation is considered generally. Huang and Edwards [11] have applied the latter to describe the hydrodynamics along with a thin-front approximation of a typical autocatalytic system. The results of this model have been compared with experimental data [9,10] and proved to be good starting points for refining theoretical considerations [13]. In a different approach, De Wit and co-workers [12,14] have used Darcy's law for fluid flow and included the full reaction term in the governing equations to allow a continuous change of density between the reactant and product mixture for both the iodate-arsenous acid and the chlorite-tetrathionate reactions.

The numerical works have shown that the pattern formation is significantly affected by the gapwidth of the Hele-Shaw cell [11,12,14], which hasn't been studied experimentally in detail. Our aim is to determine experimentally how the dispersion relation characterizing the stability of planar fronts of the chlorite-tetrathionate reaction depends upon the systematic variation of the gapwidth of the Hele-Shaw cell.

II. EXPERIMENT

Reagent-grade chemicals (Sigma, Aldrich, Reanal) were used throughout the work, except for sodium chlorite (Aldrich, tech.), which was recrystallized, as described previously [15]. The solution with composition in Table I was mixed and injected into a Hele-Shaw cell of 16 cm×12 cm area and 0.40–1.04 mm gapwidth with Plexiglas walls at temperature $25\pm1\,°C$. In some experiments one of the Plexiglas walls was replaced with an aluminum plate of the same thickness. Planar fronts were initiated either electrochemically by applying a 3 V potential difference between a pair of thin Pt-wire electrodes (0.25 mm in diameter) for 2–3 s or by placing a thin paper containing the product solution on top of the cell.

TABLE I. Composition of reactant solution.

$[K_2S_4O_6]$/M	0.005
$[NaClO_2]$/M	0.020
$[NaOH]$/M	0.001
$[Congo\ red]$/mM	0.574

*Email address: atoth@chem.u-szeged.hu

TABLE II. Increase in temperature (average ΔT_a and the maximum ΔT_m) for various gapwidths.

a/mm	ΔT_a/K	ΔT_m/K
0.40	0.28	0.53
0.51	0.34	0.54
0.59	0.33	0.52
0.71	0.51	0.78
0.81	0.67	0.87
0.91	0.68	0.95
1.04	0.73	0.94

The traveling fronts were monitored through an appropriate cutoff filter—to enhance contrast between reacted and fresh solutions—by a monochrome change-coupled device (CCD) camera connected to an MVdelta imaging card. Frames of 768×576 pixels were digitized in $0.6-3$ s intervals and processed by applying standard imaging procedures.

To determine dispersion curves for various gapwidths, a one-dimensional Fourier transformation using the FFTPACK software library from NETLIB repository has been applied with a Hann window for proper resolution of the spectra. From the initial linear regime of the time evolution of the Fourier amplitudes, the growth rates are calculated for each modes as the slopes of the straight lines of the logarithm of the amplitudes vs time curves. The results of at least six experiments have been averaged for each dispersion curve. The most unstable mode has been determined as the maximum of the parabola fitted to the middle section of the dispersion curve containing the largest growth rates. The marginal wave numbers separating the unstable modes from the stable one have been obtained from the wave numbers close to zero growth rate by fitting a straight line to the four nearest points. The dispersion curves obtained using the different initiation methods were identical within the experimental error; therefore, the electrochemical initiation was used throughout our work because of its technical simplicity.

The density change due to isothermal composition change was measured as $\Delta \rho_C = 3.8 \times 10^{-4}$ g/cm^3 previously [10]. The thermally induced density change was calculated from the temperature profiles obtained in a separate set of experiments. A thin thermocouple was placed in the solution and the temperature was measured and found to show a sudden rise at the front—in the range of $0.5-1.0$ K with increasing gapwidth but considerably less than the adiabatic 2.4 K [10]—followed by a significantly slower drop with rates increasing on decreasing the gapwidth. In cells with an aluminum wall on one side the temperature rise was 0.14 K for the thickest cell. The change in temperature was characterized both with the maximum of the temperature profiles (ΔT_m) and with the average temperature rise (ΔT_a) calculated for the product solution within the convectional length scale (see Table II). The density change due to the thermal expansion was approximated in dilute solutions from that of water as -2.57×10^{-4} g/(cm^3 K)ΔT. The observed temperature profiles were in accordance with the exothermicity of the chlorite oxidation of tetrathionate [10].
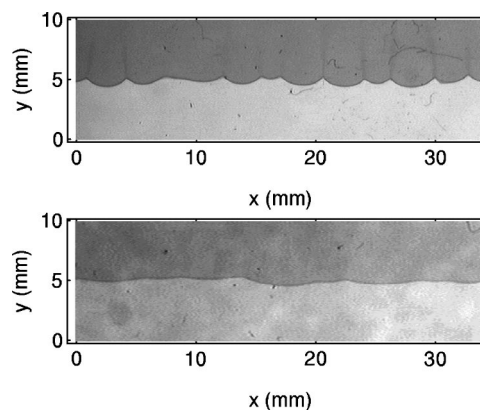

FIG. 1. Images of fronts propagating downwards for $a = 0.81$ mm at $t = 54$ s (top) and for $a = 0.40$ mm at $t = 184$ s (bottom). Darker regions represent the denser product solution and lighter the reactant.

III. RESULTS AND DISCUSSION

Under our experimental conditions the product solution is denser than the reactant one; therefore, downward propagating planar fronts lose stability, leading to cellular structures shown in Fig. 1. In the opposite orientation, however, fronts propagating upwards are stable as illustrated by the dispersion curves of Fig. 2, since for every wave number the initial perturbations decay in time. The downward propagating fronts at the same time exhibit positive growth rates for a finite regime of wave numbers indicating that the random noise within the initially planar front is amplified by convection. The patterns evolve simultaneously (see Fig. 3)—similar to diffusion-driven lateral instabilities of reaction-diffusion systems [16]—with an average wavelength of 3.5 mm increasing to 5 mm on decreasing the gapwidth and with an amplitude decreasing drastically, as shown in Fig. 1. While the upward propagating front settles at the propagation velocity of the pure reaction-diffusion front, in the buoyantly unstable orientation not only fingers appear but also the velocity of propagation increases as the arising convection enhances the mixing of the reacting species. The initial growth of fingers monotonously slows down as the gapwidth decreases although the characteristic wavelength only starts to increase at a smaller gapwidth of 0.6 mm.
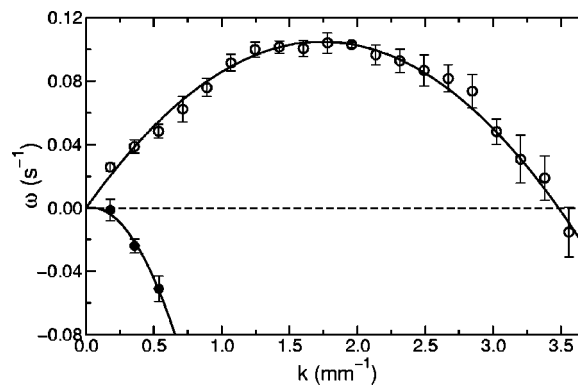

FIG. 2. Dispersion curves for downward propagating ($\bigcirc$) and upward propagating ($\bullet$) fronts with $a = 1.04$ mm gapwidth.
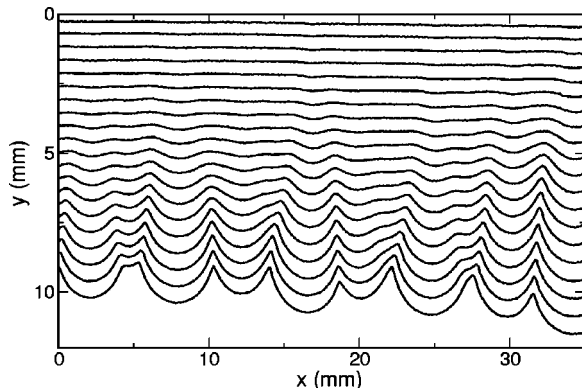
FIG. 3. Evolution of fingers for an initially planar front propagating downwards with $a = 0.81$ mm and $\Delta t = 4$ s.

From the initial regime of the temporal evolution of the fingers (e.g., from data corresponding to front profiles up to 35 s in Fig. 3), the dispersion curves have been determined for various gapwidths, as illustrated in Fig. 4. The observed average wavelength always lies in the vicinity of the mode with the highest growth rate confirming that the initial pattern is governed by the most unstable mode. The range of instability appears unchanged and hence the marginal wave number is constant down to a gapwidth of 0.6 mm and then decreases on further decreasing the gapwidth. There is no significant change or trend within the experimental error in the ratio of $k_0/k_m = 2.04 \pm 0.04$, similar to that in the study of orientation dependence [10]. We have determined the characteristics of the most unstable mode as a function of gapwidth shown in Fig. 5, which indicates that Darcy's law may be applicable below 0.6 mm. In the iodate-arsenous acid reaction [9] similar limit has been observed, since the change in density and the size of the initial fingers have the same magnitude for both reactions [9]. In thicker Hele-Shaw cells, the wave number of the most unstable mode becomes almost constant (~ 1.7 mm^{-1}) in accordance with the visually observed characteristic wavelength. The growth rate of the most unstable mode, however, exhibits a continuous increase in the entire range of gapwidth studied although with consid-
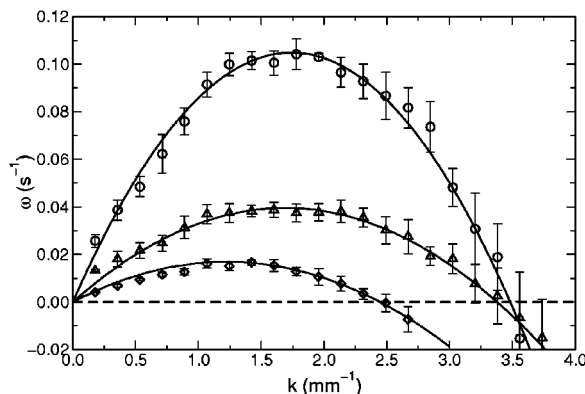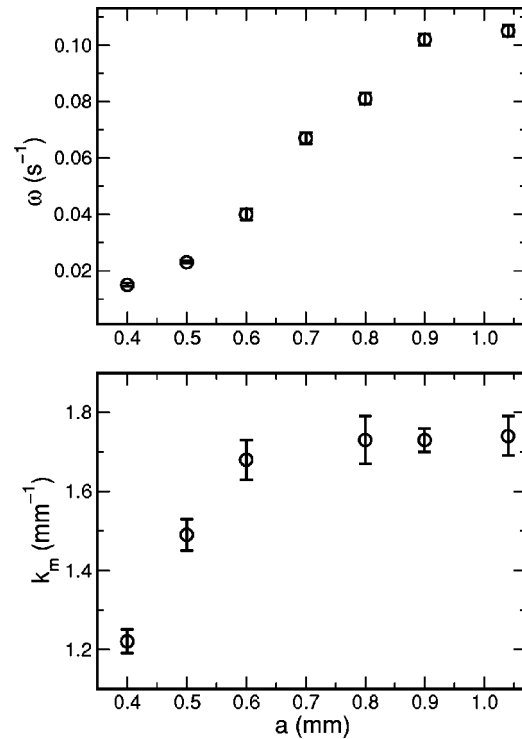

FIG. 5. The growth rate and the wave number of the most unstable mode as a function of the gapwidth of the Hele-Shaw cell.

erably smaller rate above $a = 0.9$ mm, which is the general behavior when the fluid flow is described by the Navier-Stokes equation [9,11].

In these experiments the walls of Hele-Shaw cells were made of Plexiglas, which may act as an insulator in the short time scale of the experiments, therefore the contribution of small rise in temperature to the overall change in density may not be neglected even though the gaps utilized are relatively thin. Separate experiments have therefore been carried out where one of the walls is replaced by a conducting aluminum wall that enhances the heat removal, resulting in a smaller temperature increase and hence a larger net density increase. The dispersion curves of Fig. 6 obtained for the
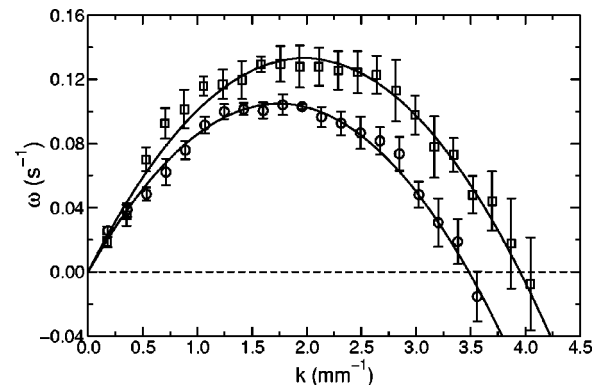

FIG. 4. Dispersion curves for $a = 0.40$ mm ($\diamond$), $a = 0.59$ mm ($\triangle$) mm, and $a = 1.04$ mm ($\bigcirc$). The solid lines correspond to the fitted parabolas with zero origin to determine the fastest growing mode.

FIG. 6. Dispersion curves for Hele-Shaw cells with Plexiglas walls ($\bigcirc$) and for cells with Plexiglas and aluminum walls ($\square$) with $a = 1.04$ mm. The solid lines correspond to the fitted parabolas with zero origin to determine the fastest growing mode.

thickest cell ($a = 1.04$ mm) demonstrate the significance of the thermal contribution to the density change. The region of instability increases when the aluminum wall is used, resulting in a 27% higher growth rate and a 14% larger wave number for the most unstable mode. Experiments with thinner cells show that the region described by Darcy's law may increase up to 0.7 mm at the concentrations listed in Table I as a result of the smaller rise in temperature. The temperature dependence of the viscosity of the solvent water predicts a small decrease in viscosity across the chemical front, which, in principal, could destabilize planar fronts [17]. Its contribution to the instability is, however, negligible with respect to that of the net density change; therefore, viscous fingering plays no role in this system.

Finally we can conclude that simple convection arises in autocatalytic fronts of the chlorite-tetrathionate reaction under the applied conditions, since upward propagating planar fronts are stable at the entire range of gapwidth examined. The convective instability induced by solutal effects may be described by Darcy's law up to 0.6–0.7 mm gapwidth with the Navier-Stokes equation being necessary above this limit. Upon increasing the thickness of the solution not only the nature of fluid motion changes but also the effectiveness of the heat removal of the system. For an exothermic reaction the latter results in an increasing temperature rise at the front, which decreases the overall density change via the thermal expansion of the solution. We believe that in this range the consideration of the temperature change, i.e., the inclusion of energy balance, is necessary in modeling equations for obtaining quantitative agreement with experimental observations. For qualitative description, the total density change should contain the solutal and thermal component approximated from the average temperature built up in the wake of the front.

[1] I.R. Epstein and J.A. Pojman, *An Introduction to Nonlinear Dynamics: Oscillations, Waves, Patterns, and Chaos* (Oxford University Press, Oxford, 1998).

[2] Gy. Bazsa and I.R. Epstein, J. Phys. Chem. **89**, 3050 (1985).

[3] I. Nagypál, Gy. Bazsa, and I.R. Epstein, J. Am. Chem. Soc. **108**, 3635 (1986).

[4] J.A. Pojman, I.R. Epstein, T.J. McManus, and K. Showalter, J. Phys. Chem. **95**, 1299 (1991).

[5] J. Masere, D.A. Vasquez, B.F. Edwards, J.W. Wilder, and K. Showalter, J. Phys. Chem. **98**, 6505 (1994).

[6] H.S. Hele-Shaw, Nature (London) **58**, 34 (1898).

[7] I.P. Nagy, A. Keresztessy, J.A. Pojman, Gy. Bazsa, and Z. Noszticzius, J. Phys. Chem. **98**, 6030 (1994).

[8] M.R. Carey, S.W. Morris, and P. Kolodner, Phys. Rev. E **53**, 6012 (1996).

[9] M. Böckmann and S.C. Müller, Phys. Rev. Lett. **85**, 2506 (2000).

[10] D. Horváth, T. Bánsági, Jr., and Á. Tóth, J. Chem. Phys. **117**, 4399 (2002).

[11] J. Huang and B.F. Edwards, Phys. Rev. E **54**, 2620 (1996).

[12] A. De Wit, Phys. Rev. Lett. **87**, 054502 (2001).

[13] J. Martin, N. Rakotomalala, D. Salin, and M. Böckmann, Phys. Rev. E **65**, 051605 (2002).

[14] J. Yang, A. D'Onofrio, S. Kalliadasis, and A. De Wit, J. Chem. Phys. **117**, 9395 (2002).

[15] Á. Tóth, D. Horváth, and A. Siska, J. Chem. Soc., Faraday Trans. **93**, 73 (1997).

[16] D. Horváth and Á. Tóth, J. Chem. Phys. **108**, 1447 (1998).

[17] G.M. Homsy, Annu. Rev. Fluid Mech. **19**, 271 (1987).